

Short Communication:**Effect of Sensitive pH on Hydroxyapatite Properties Synthesized from Chicken Eggshell**

Ferli Septi Irwansyah^{1,2}, Azhari Yusuf¹, Diana Rakhmawaty Eddy¹,
Risdiana Risdiana³, and Atiek Rostika Noviyanti^{1*}

¹Department of Chemistry, Faculty of Mathematics and Natural Sciences, Universitas Padjadjaran,
Jl. Raya Bandung-Sumedang Km. 21 Jatinangor, Sumedang 45363, West Java, Indonesia

²Department of Chemistry Education, UIN Sunan Gunung Djati Bandung
Jl. A.H. Nasution No. 105, Bandung 40614, West Java, Indonesia

³Department of Physics, Faculty of Mathematics and Natural Sciences, Universitas Padjadjaran,
Jl. Raya Bandung-Sumedang Km. 21 Jatinangor, Sumedang 45363, West Java, Indonesia

* Corresponding author:

email: atiek.noviyanti@unpad.ac.id

Received: February 10, 2022

Accepted: April 6, 2022

DOI: 10.22146/ijc.72959

Abstract: The hydrothermal method has effectively synthesized hydroxyapatite (HA). This study aimed to analyze the effect of pH on the properties (purity, crystallinity, and size) of HA crystals. HA synthesis of chicken eggshells was carried out using the hydrothermal method at temperatures of 230 °C with pH 9 and 9.34. The characteristics of HA are determined by XRF, XRD, FTIR, and TEM. The composition of the most significant compound obtained from the results of XRF analysis is CaO (97.5%). The XRD analysis showed that the purity of HA with pH 9.00 and 9.34 obtained was 97.8 and 96.6%, with the crystallinity of 56.46 and 56.96%. It was also obtained that the size of crystal HA was 21.8 and 15.7 nm for samples synthesized at pH 9.00 and 9.34. The results showed that the purity and size of HA were affected by differences in the pH synthesis and were relatively the same for its crystallinity which directly affects the value lattice parameter. The properties of HA produced by the hydrothermal method have met the criteria for biomedical applications.

Keywords: crystal structure; eggshells; hydrothermal; pH; XRD

■ INTRODUCTION

The advancement of clinical materials has been a significant examination center for decades, particularly for use in skeletal fix and reconstructive medical procedures [1]. Bioceramic is one of the most encouraging insert materials because of its likeness in arrangement with bone [2]. Specifically, calcium phosphate (CaP)-based bioceramic has been utilized as embed materials because of its superb compound properties and biocompatibility with hard tissues [3]. HA with general synthetic recipe $\text{Ca}_{10}(\text{OH})_2(\text{PO}_4)_6$ has drawn in extensive consideration as one of the most mind-blowing CaP-based bioceramics for use in the remaking of the skeleton [4]. HA contains most

inorganic parts found in the human bone and has a solid fondness for having tissues [5].

Furthermore, CaO is generated as a side product when high Ca/P reactant ratios are employed to make HA. The addition of CaO reduces the surface area of the composite. The reduced surface area is undesirable for the powder component of Calcium phosphate cement (CPC) since the presence of silica on the composite surface, and the composite's decreased surface area diminishes the bioactivity of HA [6]. Biocompatibility is a critical feature of 3D scaffolds designed for biomedical purposes. Furthermore, the 3D scaffolds must be biocompatible with the surrounding cells [7].

HA can be made from various raw materials of natural origin, such as limestone, eggshells, coral, and seashells. The primary material is a source of calcium in the form of CaCO_3 compounds with 94–97% [8]. The raw materials commonly used to produce HA can be obtained from various inorganic sources or natural materials [9–10]. Several types of cheap and abundant natural biological resources, such as eggshells [11], fish bones [9], seashells [8], and plants [12], have been studied by many researchers [13]. In practice, the researcher tries to reduce the cost of HA synthesizing [14]. The reduction of cost uses the calcium source from waste [11]. However, some waste should not be used because they are in the ecology cycle [13]. For example, seashells may be the habitat of tiny sea animals, and the coral reef is necessary for fish and some animals in the deep sea. If this waste is used, the environment or ecology may be damaged. Therefore, seashells and coral reefs should not be used for HA synthesizing [15]. However, bovine one and eggshell also can be used [16]. There are wastes from households that are very cheap and safe when used in HA synthesizing [17–18].

HA with raw materials from chicken eggshells and diammonium hydrogen phosphate has been synthesized using the wise drop precipitation [18–19] and the hydrothermal method [20]. The yield from the wise drop precipitation method is 74.74% [21]. Meanwhile, the yield produced by the hydrothermal method is 75% [20]. Although the yield is relatively the same, the hydrothermal method uses a lower temperature than the precipitation method (precipitation-wise drop=1000 °C and hydrothermal 230 °C). However, the Ca/P ratio of hydrothermal synthesis was 2.29 higher than the standard Ca/P HA ratio of 1.67. Based on these results, the optimum conditions for the synthesis were determined, including varying the temperature and pH of the reaction in hydrothermal synthesis [19,22–23].

The phase composition, crystallization, microstructure, particle size, mechanical properties, and thermal stability of HA strongly depend on the conditions and techniques utilized during the synthesis [24]. Among the conditions during the HA synthesis process, the pH value is the essential factor in determining the shape of

HA particles [25–26]. For example, Li et al. [27] found HA with a spherical shape at particle sizes between 20 and 30 nm formed at pH 10 and 11. At pH 8 to 9 intervals, a needle-like HA 0.25 micrometers in length was produced [26]. Another result also showed that spherical crystallites with a diameter of 1.5–8 μm could be produced when the pH of the sol-gel was increased to 8. Besides that, finer spherical HA particles with a diameter of about 0.3–1.0 μm were observed at pH 12. As a result, developing a simple, low-cost, and quick synthesis strategy for producing nano-sized pure HA is critical. The pH of the reaction is critical in determining the particle size and form of HA. A well-formed needle-like HA particle with dimensions of 10–15 nm width and 60–80 nm length was generated at pH 10. However, raising the pH resulted in the formation of more spherical nanoparticles.

The temperature and pH parameters of the synthesis affect the character of HA using hydrothermal at a temperature of 120 °C and pH 9 [24]. Based on another research, crystal shape is influenced by variations in the pH of the synthesis [28]. Differences in HA characters are a guide for variations in HA applications reported in several previous studies [22,29–32]. Acidic conditions during hydrothermal synthesis of HA powder produce spherical-shaped particles. In contrast, an increase in the pH of the feedstock causes anisotropic growth. It increases the aspect ratio of crystals, resulting in higher nucleation rates for HA crystals under alkaline conditions [33].

The mechanism of HA synthesis as a function of pH has been studied [24]. Alkaline conditions (around pH 9) are the choice to observe the effect because pure HA shows good stability at pH values of 9–10 and optimum at pH 9 but will degrade slowly at low pH levels (acid conditions) [34]. A slight change in pH can affect the characteristics and properties of HA [35]. Therefore, the pH sensitivity will be more effectively visible if the effect is observed at the optimum pH interval whose values are not too far apart. This study focuses on synthesizing HA using chicken eggshell waste as a source of calcium at pH 9.00 and 9.34 through the hydrothermal method. The effects of pH on yield, purity,

crystallinity, crystal shape, and crystal size were examined.

■ EXPERIMENTAL SECTION

Materials

The ingredients used were distilled water (H_2O), 100% Merck glacial acetic acid (CH_3COOH), chicken eggshells, and diammonium hydrogen phosphate ($(\text{NH}_4)_2\text{HPO}_4$) p.a. Merck.

Instrumentation

The tools used include glassware, autoclave, cup, FTIR (PerkinElmer Spectrum 100), alumina cake, TEM (JEOL JEM-1400plus TEM Single tilt holder TEM Grid Cu 400 mesh), XRD (PANalytical X'PERT PRO series) PW 3040/x0), XRF (Rigaku Nex CG), crucibles, analytical balance, oven, stirrer, furnace, and pH meter.

Procedure

The methods used include calcining chicken eggshells to obtain CaO , analysis using XRF, synthesis of HA by hydrothermal method, analysis using XRD, analysis using FTIR, and analysis using TEM.

Chicken eggshell calcination

The chicken eggshell waste obtained (115.9595 g) is cleaned of residual dirt and membranes using distilled water. The cleaned chicken eggshells were left in the open air for 24 h. The dried eggshell waste is then ground with a planetary ball mill to obtain a size that passes 100 mesh. The fine chicken eggshell powder was calcined using a furnace at a temperature of 1000 °C for 5 h, and the rate of temperature increase was 15 °C/min. Therefore, the obtained results in a white powder which is CaO [36]. For the elemental analysis, the chemical composition of calcined chicken eggshell was analyzed using an X-ray fluorescence spectrometer (XRF) [Rigaku NEX CG (CG 1240)] with 50 kV voltage, 4 mA current, and 200 W power at roughly 20 °C and regulated humidity.

HA synthesis

CaO powder from calcined chicken eggshells (57.4826 g) was added with 50 mL distilled water and 3.9467 g diammonium hydrogen phosphate with a mole ratio of Ca:P 1.67. Then the initial pH was measured, and

glacial acetic acid (CH_3COOH 0.1 M) was added until a pH of 9.00 (the procedure is repeated for pH 9.34). After that, the mixture was put into an autoclave and heated in an oven at 230 °C (HA 230) for 48 h. Furthermore, the HA crystals are decanted to be separated from the solution. The crystals obtained were dried in an oven at 110 °C for 2 h [37].

XRD analysis

XRD analysis was performed to identify the HA crystal lattice of chicken eggshells. The synthesized crystals were analyzed by XRD using $\text{CuK}\alpha$ radiation at an angle of 2θ from 20° to 60°. The diffractogram was analyzed using High Score Plus software to determine the purity, crystallinity, and crystal size.

FTIR analysis

Analysis to determine the functional groups of HA uses the potassium bromide (KBr) pellet technique. The pellet was obtained by mixing the finely ground sample with KBr powder using a mortar and agate vessel. The fine powder was then in the form of pellets measuring 1.24 cm by pressing 5 tons for 30 min. These fine powder pellets are mounted in cells and placed in the sample beam path of the FTIR apparatus. The results obtained are the IR spectrum. The IR spectrum was analyzed using SpectraGryph software to determine the peaks of the spectrum.

TEM analysis

TEM was used to determine the shape of HA particles by dispersing 1 mg of HA in 1 mL of isopropanol. The obtained TEM micrographs were analyzed using ImageJ software.

■ RESULTS AND DISCUSSION

The shells of calcined chicken eggs were analyzed using XRF, which aims to determine the eggshell content. The results of the XRF analysis of calcined chicken eggshells are shown in Table 1.

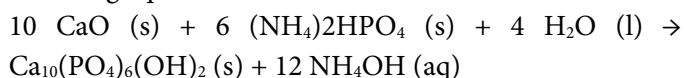
The calcination results of chicken eggshells were analyzed using XRF to determine levels of CaO . It has an effect on stoichiometry for HA synthesis. The CaO content obtained from the calcination is about 97.5%, and there are other components such as magnesium, iron,

Table 1. Composition of calcined chicken eggshells using XRF

Component	Composition (%)
MgO	1.1300
Fe ₂ O ₃	0.3680
CuO	0.0192
P ₂ O ₅	0.4060
SO ₃	0.2600
Al ₂ O ₃	0.1770
CaO	97.500
SiO ₂	0.1770

copper, phosphorus, sulfur, aluminium, and silica in the form of oxides. CaO content is obtained from the decomposition process of CaCO₃, which is the main component in chicken eggshells.

HA was synthesized using the hydrothermal method at temperatures of 230 °C for 48 h with various pH (9.00 and 9.34). This HA synthesis reaction corresponds to the following equation:



Based on the study results, the yield of HA 230 was 78.77%. The obtained yield could be affected by the unreacted reactants and other residues in CaO from chicken eggshells that reacted with (NH₄)₂HPO₄. The synthesis of HA from chicken eggshells using the wise drop precipitation method obtained optimum results at a sintering temperature of 1000 °C for 5 h with a yield of 74.74%. Based on this study, the yield of HA from the hydrothermal method was higher than that of the wise drop precipitation method [19].

Synthesis HA using the hydrothermal method with a calcium source from chicken eggshells and a phosphate source from diammonium hydrogen phosphate without adjusting the pH resulted in a yield of 75% [20]. Based on the research conducted, an increase in yield of 3.77%, proving that pH affected the yield obtained. The effect of the pH can be caused by the more effective contact between reactants occurring at pH 9. The factors that affect the yield include the effectiveness of contact between reactants, the ratio between reactants, temperature and reaction time, and the stage of purification of reaction products [38]. In this

investigation, CH₃COOH was utilized to modify the pH, which increases the concentration of OH⁻ ions throughout the synthesis process. Supersaturation of OH⁻ ions at the interface might interfere with the actions of OH⁻ ions on the crystal facets, influencing their development rates [39]. The mobility of Ca²⁺ and PO₄³⁻ ions in the precursor solution is restricted by a high concentration of OH⁻ ions at a high pH value. The absorption of OH⁻ ions at the various crystal facets is thought to change their surface energy, resulting in crystal growth with varying morphologies and sizes [24].

The XRD HA 230 pH 9.00 data were compared with the XRD 230 pH 9.34 data. The results of the analysis can be seen in Fig. 1.

The highest peak of HA 230 at pH 9.34 was at $2\theta = 31.7726^\circ$. The crystal structure of HA obtained from all reaction conditions is hexagonal with a *P* 63/*m* space group. The XRD data is then processed using High Score Plus software. The purity of HA 230 at pH 9.34 was 96.6%, with impurities in the Whitlockite phase of 3.4%. While HA 230 pH 9 has a purity of 97.8% with impurities in the form of Ca(OH)₂ of 1.4%, and the TCP phase with a percentage of 0.8%. The difference in purity is due to the influence of pH on the synthesis of HA in the hydrothermal method. The percentage of crystallinity of HA 230 at pH 9.34 was 56.96%. Compared with HA 230 at pH 9 (crystallinity = 56.46%), the percentage of

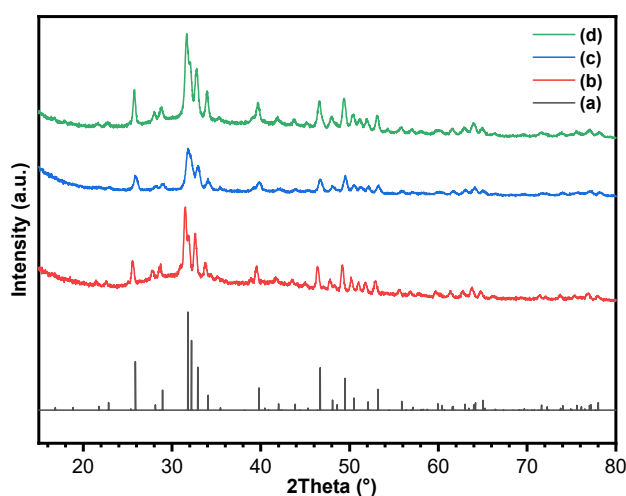


Fig 1. (a) Diffractogram images of ICSD 98-016-9498, (b) commercial HA, (c) HA 230 pH 9.34, and (d) HA 230 at pH 9.00

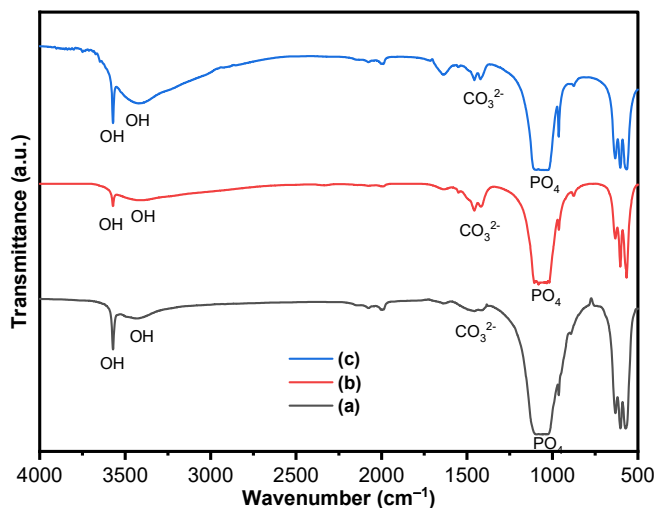


Fig 2. (a) IR Spectrum images of commercial HA, (b) HA 230 at pH 9.34, and (c) HA 230 at pH 9.00

crystallinity obtained is relatively the same. This finding proves that the relative pH does not affect the crystallinity of the obtained HA [24].

Meanwhile, the crystal size of HA 230 at pH 9.34 was 15.7 nm, while HA 230 at pH 9 had a crystal size of 21.8 nm. It is known that pH affects the crystal size and morphology of the HA [28]. The crystallite size was found to decrease monotonically with the increase and associated with the increase in the nucleation rate of the crystals, thus reaching a high concentration of the solute (supersaturation) [24]. In addition, in hydrothermal synthesis, the product's formation and stability are influenced by reaction conditions such as temperature, pressure, reagent concentration, and pH [40].

The presence of carbonates is due to the reaction between HA and CO₂ present in the atmosphere during preparation [41]. While the O–H groups identified at wavenumbers 1638 and 3433.5 cm⁻¹ indicate that the sample still contains water [24,42]. While the band at wave number 3644.0 cm⁻¹ is the stretch of the OH group on the Ca(OH)₂ molecule [37].

Fig. 2 shows that HA 230 at pH 9.34 can be seen from the presence of a band at wavenumbers 475.6, 565.7, 602.8, 963, 10043, and 1091 cm⁻¹. P–O vibrations in the phosphate group and the wavenumber of 632.5 and 3572 cm⁻¹ have O–H buckling and strain. In addition, the band at wavenumbers 877.4, 1402, and 1457 cm⁻¹ contain a CO₃²⁻ group. Meanwhile, the O–H group identified at

wavenumber 1642 cm⁻¹ indicates that the sample still contains water. The transmittance of the CO₃²⁻ group and the OH group of HA 230 pH 9.34 was lower than that of HA 230 pH 9. The observed transmittance indicates the interaction of HA with CO₂ that occurred because the sample preparation of HA 230 pH 9 was longer than HA 230 pH 9.34. In addition, the water-bound to HA 230 at pH 9 was more due to the lack of drying time of the sample after synthesis, so it was not sufficient to evaporate all the water in the sample. The data from the FTIR analysis of the effect of temperature and pH can be seen in Table 2.

TEM analysis was performed to determine the shape of HA particles produced at pH 9. The results of the TEM HA analysis are shown in Fig. 3.

Fig. 3 is a TEM micrograph of HA, which was analyzed using ImageJ software. It can be seen that HA has an irregularly elongated/rectangular tubular structure [43]. This rod-like structure indicates a restriction on the growth of HA particles caused by an increase in pH so that the concentration of H₂O increases in the solution [44]. In addition, the particle size

Table 2. FTIR analysis results of HA synthesis

Functional group	HA commercial	HA 230 at pH 9	HA 230 at pH 9.34
PO (HA)	473.4 571.7 602.1 962.9 1031 - 1091 2002 2077	473.7 566.8 602.8 963.1 1031.1 - 1091.1 2002 2077	473.2 566.6 602.8 962.4 1018 - 1106 1989 -
OH (HA)	631.4 3571	632.2 3571.3	632.4 3571
PO (TCP)	-	-	-
OH Ca(OH) ₂	-	-	-
Free OH		1637 3421.9	1634 3401
CO ₃ ²⁻	891.4 1413 1457	875.2 1421.0 1456.9	874.5 1418 1457

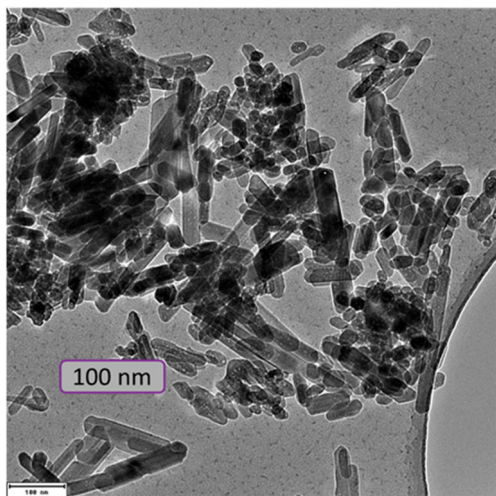


Fig 3. TEM micrograph of HA 230

Table 3. The particle size of synthesized HA

Particle size	HA 230
Mean	26.62 nm
Standard Deviation	9.22 nm
Min	17.50 nm
Max	43.60 nm

of HA 230 pH 9 is shown in Table 3.

The TEM analysis showed that the HA produced from chicken eggshell waste using the hydrothermal method had a nanoparticle size (26.62 nm). Thus, it can be concluded that the resulting HA has the potential to be used in several applications, including in the biomedical field [45].

■ CONCLUSION

This research effectively produced pure HA from chicken eggshell waste using the hydrothermal method. All experimental findings demonstrated a relationship between synthesis circumstances such as feedstock and pH levels (9.00 and 9.34). The production of HA crystals in the synthesized samples was verified by XRD and FTIR examination at pH values of 9.00 and 9.34. HA particles with irregular elongated/rectangular tubular structures were obtained at pH 9 with an average size of 26.62 nm. It was discovered that the adsorption of OH⁻ ions might be used to control the competition between crystal nucleation and crystal development of HA particles. HA at pH 9.34 had a higher crystallinity than at pH 9.00. At the same time, the crystal size and purity were higher at

pH 9.00 compared to pH 9.34. Furthermore, pH affects the particle shape of HA.

■ ACKNOWLEDGMENTS

The authors would like to convey sincere gratitude to the Directorate General of Islamic Education, Ministry of Religious Affairs, through LITAPDIMAS Number 6807 of 2021 for financial support for this research. This work is also partially supported by the Academic Leadership Grant of Universitas Padjadjaran 2021 no. 1959/UN6.3.1/PT.00/2021.

■ AUTHOR CONTRIBUTIONS

Azhari Yusuf experimented, Atiek Rostika Noviyanti analyzed the characterization, and Ferli Septi Irwansyah wrote and revised the manuscript with support from Risdiana and Diana Rakhmawaty Eddy. All authors agreed to the final version of this manuscript.

■ REFERENCES

- [1] Qaid, T.H., Ramesh, S., Yusof, F., Basirun, W.J., Ching, Y.C., Chandran, H., and Krishnasamy, S., 2019, Micro-arc oxidation of bioceramic coatings containing eggshell-derived hydroxyapatite on titanium substrate, *Ceram. Int.*, 45 (15), 18371–18381.
- [2] Sopyan, I., Pusparini, E., Ramesh, S., Tan, C.Y., Ching, Y.C., Wong, Y.H., Abidin, N.I.Z., Chandran, H., Ramesh, S., and Bang, L.T., 2017, Influence of sodium on the properties of sol-gel derived hydroxyapatite powder and porous scaffolds, *Ceram. Int.*, 43 (15), 12263–12269.
- [3] Ramesh, S., Natasha, A.N., Tan, C.Y., Bang, L.T., Ramesh, S., Ching, C.Y., and Chandran, H., 2016, Direct conversion of eggshell to hydroxyapatite ceramic by a sintering method, *Ceram. Int.*, 42 (6), 7824–7829.
- [4] Ramesh, S., Jeffrey, C.K.L., Tan, C.Y., Wong, Y.H., Ganesan, P., Ramesh, S., Kutty, M.G., Chandran, H., and Devaraj, P., 2016, Sintering behaviour and properties of magnesium orthosilicate-hydroxyapatite ceramic, *Ceram. Int.*, 42 (14), 15756–15761.

- [5] Medeiros, E.L.G., Gomes, D.S., Santos, A.M.C., Vieira, R.H., de Lima, I.L., Rocha, F.S., Castro-Filice, L.S., Medeiros, E.S., Neves, G.A., and Menezes, R.R., 2021, 3D nanofibrous bioactive glass scaffolds produced by one-step spinning process, *Ceram. Int.*, 47 (1), 102–110.
- [6] Windarti, T., Widjijono, W., and Nuryono, N., 2020, Deposition of hydroxyapatite on silica made from rice husk ash to produce the powder component of calcium phosphate cement, *Indones. J. Chem.*, 21 (3), 588–597.
- [7] Nurlidar, F., and Kobayashi, M., 2019, Succinylated bacterial cellulose induce carbonated hydroxyapatite deposition in a solution mimicking body fluid, *Indones. J. Chem.*, 19 (4), 858–864.
- [8] Ali, A.F., Alrowaili, Z.A., El-Giar, E.M., Ahmed, M.M., and El-Kady, A.M., 2021, Novel green synthesis of hydroxyapatite uniform nanorods via microwave-hydrothermal route using licorice root extract as template, *Ceram. Int.*, 47 (3), 3928–3937.
- [9] Ramesh, S., Loo, Z.Z., Tan, C.Y., Chew, W.J.K., Ching, Y.C., Tarlochan, F., Chandran, H., Krishnasamy, S., Bang, L.T., and Sarhan, A.A.D., 2018, Characterization of biogenic hydroxyapatite derived from animal bones for biomedical applications, *Ceram. Int.*, 44 (9), 10525–10530.
- [10] Gergely, G., Wéber, F., Lukács, I., Tóth, A.L., Horváth, Z.E., Mihály, J., and Balázsi, C., 2010, Preparation and characterization of hydroxyapatite from eggshell, *Ceram. Int.*, 36 (2), 803–806.
- [11] Ho, W.F., Hsu, H.C., Hsu, S.K., Hung, C.W., and Wu, S.C., 2013, Calcium phosphate bioceramics synthesized from eggshell powders through a solid state reaction, *Ceram. Int.*, 39 (6), 6467–6473.
- [12] Indira, J., and Sreeja, V., 2020, Synthesis of silver/hydroxyapatite/tryptophan nanocomposite particles by biological method, *Mater. Today: Proc.*, 51, 1685–1689.
- [13] Akram, M., Ahmed, R., Shakir, I., Ibrahim, W.A.W., and Hussain, R., 2013, Extracting hydroxyapatite and its precursors from natural resources, *J. Mater. Sci.*, 49 (4), 1461–1475.
- [14] Ng, C.K., Ng, Z.L., Ramesh, S., Tan, C.Y., Ting, C.H., Chuah, Y.D., and Sutharsini, U., 2020, Synthesis and properties of bio-waste-based hydroxyapatite via hydrothermal process, *Materialwiss. Werkstofftech.*, 51 (6), 706–712.
- [15] Krishnan G, R., Prabhakaran, K., and George, B.K., 2021, Biogenic magnetic nano hydroxyapatite: Sustainable adsorbent for the removal of perchlorate from water at near-neutral pH, *J. Environ. Chem. Eng.*, 9 (6), 106316.
- [16] Niakan, A., Ramesh, S., Ganesan, P., Tan, C.Y., Purbolaksono, J., Chandran, H., Ramesh, S., and Teng, W.D., 2015, Sintering behaviour of natural porous hydroxyapatite derived from bovine bone, *Ceram. Int.*, 41 (2), 3024–3029.
- [17] Bee, S.L., and Hamid, Z.A.A., 2020, Hydroxyapatite derived from food industry bio-wastes: Syntheses, properties and its potential multifunctional applications, *Ceram. Int.*, 46 (11), 17149–17175.
- [18] Yusuf, A., Muhammad, N.M., Noviyanti, A.R., and Risdiana, R., 2020, The effect of temperature synthesis on the purity and crystallinity of hydroxyapatite, *Key Eng. Mater.*, 860, 228–233.
- [19] Noviyanti, A.R., Rahayu, I., Fauzia, R.P., and Risdiana, R., 2021, The effect of Mg concentration to mechanical strength of hydroxyapatite derived from eggshell, *Arabian J. Chem.*, 14 (4), 103032.
- [20] Noviyanti, A.R., Akbar, N., Deawati, Y., Ernawati, E.E., Malik, Y.T., Fauzia, R.P., and Risdiana, R., 2020, A novel hydrothermal synthesis of nanohydroxyapatite from eggshell-calcium-oxide precursors, *Heliyon*, 6 (4), e03655.
- [21] Noviyanti, A.R., Haryono, H., Pandu, R., and Eddy, D.R., 2017, Cangkang telur ayam sebagai sumber kalsium dalam pembuatan hidroksiapatit untuk aplikasi graft tulang, *Chim. Nat. Acta*, 5 (3), 107–111.
- [22] Shi, H., Zhou, Z., Li, W., Fan, Y., Li, Z., and Wei, J., 2021, Hydroxyapatite based materials for bone tissue engineering: A brief and comprehensive introduction, *Crystals*, 11 (2), 149.
- [23] Palanivelu, R., Mary Saral, A., and Ruban Kumar, A., 2014, Nanocrystalline hydroxyapatite prepared under various pH conditions, *Spectrochim. Acta, Part A*, 131, 37–41.

- [24] Goh, K.W., Wong, Y.H., Ramesh, S., Chandran, H., Krishnasamy, S., Sidhu, A., and Teng, W.D., 2021, Effect of pH on the properties of eggshell-derived hydroxyapatite bioceramic synthesized by wet chemical method assisted by microwave irradiation, *Ceram. Int.*, 47 (7), 8879–8887.
- [25] Othman, R., Mustafa, Z., Loon, C.W., and Noor, A.F.M., 2016, Effect of calcium precursors and pH on the precipitation of carbonated hydroxyapatite, *Procedia Chem.*, 19, 539–545.
- [26] Bogdanoviciene, I., Tõnsuaadu, K., Mikli, V., Grigoraviciute-Puroniene, I., Beganskiene, A., and Kareiva, A., 2010, pH impact on the sol-gel preparation of calcium hydroxyapatite, $\text{Ca}_{10}(\text{PO}_4)_6(\text{OH})_2$, using a novel complexing agent, DCTA, *Cent. Eur. J. Chem.*, 8 (6), 1323–1330.
- [27] Wang, P., Li, C., Gong, H., Jiang, X., Wang, H., and Li, K., 2010, Effects of synthesis conditions on the morphology of hydroxyapatite nanoparticles produced by wet chemical process, *Powder Technol.*, 203 (2), 315–321.
- [28] Rodríguez-Lugo, V., Karthik, T.V.K., Mendoza-Anaya, D., Rubio-Rosas, E., Villaseñor Cerón, L.S., Reyes-Valderrama, M.I., and Salinas-Rodríguez, E., 2018, Wet chemical synthesis of nanocrystalline hydroxyapatite flakes: Effect of pH and sintering temperature on structural and morphological properties, *R. Soc. Open Sci.*, 5 (8), 180962.
- [29] Bartonickova, E., Vojtisek, J., Tkacz, J., Porizka, J., Masliko, J., Moncekova, M., and Parizek, L., 2017, Porous HA/alumina composites intended for bone-tissue engineering, *Mater. Tehnol.*, 51 (4), 631–636.
- [30] Ratha, I., Datta, P., Balla, V.K., Nandi, S.K., and Kundu, B., 2021, Effect of doping in hydroxyapatite as coating material on biomedical implants by plasma spraying method: A review, *Ceram. Int.*, 47 (4), 4426–4445.
- [31] Saha, B., Yadav, S.K., and Sengupta, S., 2018, Synthesis of nano-Hap prepared through green route and its application in oxidative desulfurisation, *Fuel*, 222, 743–752.
- [32] Müller, V., Pagnier, T., Tadier, S., Gremillard, L., Jobbagy, M., and Djurado, E., 2021, Design of advanced one-step hydroxyapatite coatings for biomedical applications using the electrostatic spray deposition, *Appl. Surf. Sci.*, 541, 148462.
- [33] Toibah, A.R., Misran, F., Shaaban, A., and Mustafa, Z., 2019, Effect of pH condition during hydrothermal synthesis on the properties of hydroxyapatite from eggshell waste, *J. Mech. Eng. Sci.*, 13 (2), 4958–4969.
- [34] Narendran, P., Rajendran, A., Garhnayak, M., Garhnayak, L., Nivedhitha, J., Devi, K.C., and Pattanayak, D.K., 2018, Influence of pH on wet-synthesis of silver decorated hydroxyapatite nanopowder, *Colloids Surf., B*, 169, 143–150.
- [35] Weerasuriya, D.R.K., Wijesinghe, W.P.S.L., and Rajapakse, R.M.G., 2017, Encapsulation of anticancer drug copper bis(8-hydroxyquinoline) in hydroxyapatite for pH-sensitive targeted delivery and slow release, *Mater. Sci. Eng. C*, 71, 206–213.
- [36] Hutabarat, G.S., Qodir, D.T., Setiawan, H., Akbar, N., and Noviyanti, A.R., 2019, Sintesis komposit hidroksiapatit-lantanum oksida ($\text{HA}-\text{La}_2\text{O}_3$) dengan metode hidrotermal secara *in-situ* dan *ex-situ*, *ALCHEMY Jurnal Penelitian Kimia*, 15 (2), 287–301.
- [37] Rodríguez-Lugo, V., Salinas-Rodríguez, E., Vázquez, R.A., Alemán, K., and Rivera, A.L., 2017, Hydroxyapatite synthesis from a starfish and β -tricalcium phosphate using a hydrothermal method, *RSC Adv.*, 7 (13), 7631–7639.
- [38] Noviyanti, A.R., Hastiawan, I., Yuliyati, Y.B., Rahayu, I., Rosyani, D., and Syarif, D.G., 2017, LSO apatite-YSZ composite as a solid electrolyte for solid oxide fuel cells, *AIP Conf. Proc.*, 1848, 040001.
- [39] Qi, Y., Shen, J., Jiang, Q., Jin, B., Chen, J., and Zhang, X., 2015, The morphology control of hydroxyapatite microsphere at high pH values by hydrothermal method, *Adv. Powder Technol.*, 26 (4), 1041–1046.
- [40] Nadimpalli, N.K.V., Bandyopadhyaya, R., and Runkana, V., 2018, Thermodynamic analysis of hydrothermal synthesis of nanoparticles, *Fluid Phase Equilib.*, 456, 33–45.
- [41] Liu, J., Ye, X., Wang, H., Zhu, M., Wang, B., and Yan, H., 2003, The influence of pH and temperature

- on the morphology of hydroxyapatite synthesized by hydrothermal method, *Ceram. Int.*, 29 (6), 629–633.
- [42] Vưòng, B.X., and Linh, T.H., 2019, The extraction of pure hydroxyapatite from porcine bone by thermal process, *Metall. Mater. Eng.*, 25 (1), 47–58.
- [43] Huixia, L., Yong, L., Lanlan, L., Yanni, T., Qing, Z., and Kun, L., 2016, Development of ammonia sensors by using conductive polymer/hydroxyapatite composite materials, *Mater. Sci. Eng.*, C, 59, 438–444.
- [44] Rodríguez-Lugo, V., Karthik, T.V.K., Mendoza-Anaya, D., Rubio-Rosas, E., Villaseñor Cerón, L.S., Reyes-Valderrama, M.I., and Salinas-Rodríguez, E., 2018, Wet chemical synthesis of nanocrystalline hydroxyapatite flakes: Effect of pH and sintering temperature on structural and morphological properties, *R. Soc. Open Sci.*, 5 (8), 180962.
- [45] Varadavenkatesan, T., Vinayagam, R., Pai, S., Kathirvel, B., Pugazhendhi, A., and Selvaraj, R., 2021, Synthesis, biological and environmental applications of hydroxyapatite and its composites with organic and inorganic coatings, *Prog. Org. Coat.*, 151, 106056.